Pharmaceutics, Drug Delivery and Pharmaceutical Technology

Budesonide-Loaded Bilosomes as a Targeted Delivery Therapeutic Approach Against Acute Lung Injury in Rats

Heba F. Salem[a], Ghada Abdelsabour Moubarak[b], Adel A. Ali[a], Abeer A.A. Salama[c], Alaa H. Salama[b,d],*

[a] Department of Pharmaceutics and Industrial Pharmacy, Faculty of Pharmacy, Beni-Suef University, Beni-Suef, Egypt
[b] Department of Pharmaceutics and Industrial Pharmacy, Faculty of Pharmacy, Ahram Canadian University, 6th of October City, Cairo, Egypt
[c] Pharmacology Department, National Research Centre, Dokki, Cairo 12622, Egypt
[d] Pharmaceutical Technology Department, National Research Centre, Dokki, Cairo 12622, Egypt

ABSTRACT

Budesonide (BUD), a glucocorticoids drug, inhibits all steps in the inflammatory response. It can reduce and treat inflammation and other symptoms associated with acute lung injury such as COVID-19. Loading BUD into bilosomes could boost its therapeutic activity, and lessen its frequent administration and side effects. Different bilosomal formulations were prepared where the independent variables were lipid type (Cholesterol, Phospholipon 80H, L-alpha phosphatidylcholine, and Lipoid S45), bile salt type (Na cholate and Na deoxycholate), and drug concentration (10, 20 mg). The measured responses were: vesicle size, entrapment efficiency, and release efficiency. One optimum formulation (composed of cholesterol, Na cholate, and 10 mg of BUD) was selected and investigated for its anti-inflammatory efficacy *in vivo* using Wistar albino male rats. Randomly allocated rats were distributed into four groups: The first: normal control group and received intranasal saline, the second one acted as the acute lung injury model received intranasal single dose of 2 mg/kg potassium dichromate (PD). Whereas the third and fourth groups received the market product (Pulmicort® nebulising suspension 0.5 mg/ml) and the optimized formulation (0.5 mg/kg; intranasal) for 7 days after PD instillation, respectively. Results showed that the optimized formulation decreased the pro-inflammatory cytokines TNF-α, and TGF-β contents as well as reduced PKC content in lung. These findings suggest the potentiality of BUD-loaded bilosomes for the treatment of acute lung injury with the ability of inhibiting the pro-inflammatory cytokines induced COVID-19.

© 2022 Published by Elsevier Inc. on behalf of American Pharmacists Association.

Introduction

Budesonide (BUD) is an anti-inflammatory drug that can be classified based on the biopharmaceutics classification system (BCS) as class II. It reduces the body's natural defense response.[1] Recently, research has shown that BUD has a significant anti-inflammatory effect in the treatment of coronaviruses.[2] However, its hydrophobic nature comprises an essential hindrance in its clinical use, manifested by its low solubility/dissolution rate affecting its absorption. Thus, a proposed strategy for improving its bioavailability is its inclusion within stable lipid vesicles, bilosomes.[3]

Bilosomes comprise type of vesicular carrier composed of bile acid salts integrated within the bilayer membrane of the non-ionic surfactant molecules.[4] They are soft and flexible carriers with more efficient penetration capability.[5,6] When loaded with therapeutic agents, they enhance their absorption and, consequently their bioavailability.[5,7] Also, they are safe with no reported toxicity, which makes them suitable for drug delivery purposes.[8]

Different lipid constituents could be used for the formulation of vesicles; four types of lipids were used in this study; cholesterol, Phospholipon 80H, Lipoid S45, and L-alpha Phosphatidylcholine. Cholesterol is a widely used component for vesicles preparation with a proven efficacy in reducing vesicles size and increasing vesicles entrapment efficiency.[9−12] Specifically, cholesterol improved the stability of bilosomes, decreased their vesicular size, and enhanced their entrapment efficiency.[13,14] On the other hand, Phospholipon 80H, hydrogenated Phospholipids from soybean containing 70% Phosphatidylcholine, has been reported to enhance the homogeneity of bilosomes, as when incorporated within bilosomal structures, small-sized vesicles are produced.[15] Moreover, it has the ability to enhance vesicles' penetration.[16] Also, Lipoid S45, a soybean lecithin free of fat containing 45% Phosphatidylcholine, is efficient in generating vesicles

Table 1
Mixed factorial design $4^1.2^2$ proposed for preparing and optimizing BUD-loaded bilosomal vesicular systems.

Factors (independent variables)		Levels		
Lipid type	Cholesterol	Phospholipon 80H	L-α-phosphatidylcholine	Lipoid S45
Bile salt type	Na cholate		Na deoxycholate	
Drug concentration	10 mg		20 mg	
Factors (dependent variables)		Constraints		
Y1:Vesicle size (VS)		Minimize		
Y2:Entrapment efficiency (EE)		Maximize		
Y3:Release Efficiency (RE)		Maximize		

with high penetrating ability.[16,17] Whereas, L-alpha phosphatidylcholine is known to maintain the membrane permeability.[18]

Potassium dichromate (PD) contains chromium (Cr) which can induce acute lung injury (ALI) and is accompanied by high morbidity and mortality.[19] Cr is widely used in industries released in the form of toxic compounds such as hexavalent form (chromium VI) causing carcinogenic, mutagenic, teratogenic effects[20,21] and multiple organ failure such as lung[19] and kidney via inflammatory cytokine NF-$\kappa\beta$.[22] Also in lung, Cr generates reactive oxygen species (ROS) and inflammatory cytokine TGF-β inducing acute lung injury. Furthermore, protein kinase C (PKC) contributes to the generation of ROS such as superoxide anions and stimulates NADPH oxidase (NOX) provoking acute injury in lung.[23] Coronavirus causes severe destruction to the respiratory tract, specifically, the lung. When COVID-19 gets into the respiratory tract, it results in a mild or highly acute respiratory syndrome associated with pro-inflammatory cytokines release. Accordingly, the disease severity is related to the cytokine storm production[24] which causes high mortality risk.[24,25] Thus, an ideal strategy to overcome the symptoms is to target drugs to pro-inflammatory cytokines.[26,27]

The aim of this study is to encapsulate BUD within bilosomal vesicles aiming to increase its therapeutic efficacy for targeted pulmonary delivery. Then, BUD-loaded bilosomes were investigated to relieve lung inflammation. Bilosomal formulations were analyzed according to a mixed factorial experimental design with the aid of Design-Expert® software. Accordingly, the selected optimized formulation was assessed for its *in vivo* performances using Wister albino male rats model to investigate its anti-inflammatory effect against acute lung injury that induced by PD via measuring the following cytokines inflammatory mediators: Transforming growth factor beta (TGF-β), and tumor necrosis factor alpha (TNF-α) as well as PKC.

Material and Methods

Materials

Budesonide (BUD) was kindly acquired from Jayco chemical industries (INDIA), cholesterol (CSTRL), L-alpha phosphatidylcholine (L-α-PC) (Soybean phosphatidylcholine with 33% phosphatidylcholine), span 60, sodium cholate (SC), Dialysis membrane with a molecular weight cut off of 14,000 DA, and potassium dichromate (PD) were brought from Sigma Aldrich (St. Louis, MO). Phospholipon 80H (P 80H) and Lipoid S45 (L S45) were kindly obtained from Lipoid, Switzerland. Sodium deoxycholate (SDC) was acquired from BDH (England). Protein kinase C (PKC), and tumor necrosis factor alpha (TNF-α) were purchased from specific SunLong, China, ELISA kits, transforming growth factor beta (TGF-β) was obtained from SinoGeneclone, China, ELISA kits. Potassium dihydrogen phosphate and sodium dihydrogen phosphate were of analytical grade. Chloroform, and methanol were bought from Fisher scientific for chemicals with HPLC grade, UK. Ethanol was bought from International company for sup & med Industries, Egypt.

Methods

Fabrication of BUD-Loaded Bilosomal Formulations

Experimental design. Mixed-factorial experimental design was adopted to prepare different BUD-loaded bilosomes using Design-Expert® software (version 10.0.8.0 32-bit) (Tables 1 and 2). The studied factors can be listed as follows; drug concentration (10, 20 mg) coded as (A), lipid type (CSTRL, P 80H, L-α-PC, and L S45) coded as (B), and bile salt type (SC and SDC) coded as (C). The obtained formulations were characterized for vesicle size (VS) coded as (Y1), % entrapment efficiency (EE) coded as (Y2), and % release efficiency coded as (Y3) (Table 1).

Preparation of BUD-Loaded bilosomes. Thin-film hydration technique was used to prepare different BUD-loaded bilosomal formulations[28−31] with slight modification. Accurately weighed amounts (0.0965 gm) of lipid (CSTRL, P 80H, L-α- PC, or L S45), 1.1965 gm Span 60, and (10 or 20 mg) of BUD were dispersed in 10 ml organic solvent composed of methanol/chloroform (2:1) in a 250 ml round-bottomed flask by sonication (Elmasonic S 30 H, Germany). The resulting organic dispersion was gradually vaporized at 80 rpm, and 50 ± 0.5°C under vacuum for 30 min using a rotary evaporator (Heidolph, Germany) until a homogenous thin, completely dried film was obtained. The produced film was then exposed to hydration with 10 mL aqueous solution containing 0.215 gm of bile salt (SC or SDC) at the same used temperature under atmospheric pressure for another half an hour to allow the formation of a colloidal dispersion.[4,28,32] Table 2 demonstrates the composition of BUD-loaded bilosomal formulations.

Characterization of BUD-Loaded Bilosomes

Assessment of vesicles size (VS), polydispersity index (PDI), and zeta potential (ZP). Dynamic Light Scattering, integrated into a Malvern Zeta Sizer (Malvern, Germany) was used in order to measure the VS, their degree of homogeneity (PDI), and zeta potential of the prepared vesicles.[33] Before measurement, samples were appropriately diluted using de-ionized water to generate adequate scattering intensity. Diluted bilosomal suspension was placed in the sample cuvette and measured. For each sample, three independent assays were taken at a scattering angle of 90° and a temperature of 25±2°C.[34]

Determination of Entrapment Efficiency-Values. This was assessed indirectly by calculating the free amount of BUD in the colloidal dispersion. Thus, specific volume of each preparation was centrifuged under cooling (-4°C) at 15000 rpm for 60 min (Sigma 3-30KS, Germany). The separated supernatant was measured for the BUD amount spectrophotometrically at 247 nm (Jasco UV spectrophotometer V-630, Japan). The following equation was used to determine EE%[31,35]:

$$EE\ (\%) = \frac{Total\ amount\ of\ BUD - amount\ of\ free\ BUD}{Total\ amount\ of\ BUD} \times 100$$

Table 2
Composition of the prepared BUD-loaded bilosomal vesicular systems.

Formula	Type of lipid	Type of bile salt	Drug concentration(mg)
F1	Cholesterol	Na cholate	10
F2		Na deoxycholate	10
F3		Na cholate	20
F4		Na deoxycholate	20
F5	Phospholipon 80H	Na cholate	10
F6		Na deoxycholate	10
F7		Na cholate	20
F8		Na deoxycholate	20
F9	L-α-phosphatidylcholine	Na cholate	10
F10		Na deoxycholate	10
F11		Na cholate	20
F12		Na deoxycholate	20
F13	Lipoid S45	Na cholate	10
F14		Na deoxycholate	10
F15		Na cholate	20
F16		Na deoxycholate	20

Each formula was assessed in triplicate and the results were stated in the form of mean ± SD.

In vitro *BUD release study.* In brief, the obtained BUD-loaded bilosomes, after centrifugation, were placed into cellulose dialysis bags, which were then tightly closed at both ends. The cellulose dialysis bags were immersed in phosphate buffer (100 mL, pH 7.4) containing 20% v/v of absolute ethanol. The release media were kept at 37±0.5°C in a thermostatically controlled shaker (LKLAB, Korea) at 100 rpm. Sampling (2 mL) was performed at predetermined time intervals and were taken out for 72 h and exchanged with fresh medium. Samples were spectrophotometrically analyzed at 247 nm (Jasco UV spectrophotometer V-630, Japan).[36] The release experiments were performed in triplicates with the data displayed as the mean values ± SD.

The obtained in vitro BUD release data from different prepared bilosomal formulations were evaluated and the release efficiency (RE%) was calculated from the area under the release curve at time t. The parameter relates the area under the release curve to the rectangle corresponding to full drug release (100%, Y_{100}).[33] The equation used for its calculation is listed below:

$$RE\% = \frac{\int_0^t y \ x \ dt}{y_{100} \ x \ t} \times 100$$

Where y represents %BUD releases at certain time t.

Optimization and Validation of the Experimental Model

Design-Expert® software (version 10.0.8.0 32-bit) was used to analyze the collected data for the studied responses using ANOVA test. Design-Expert® software picks the suitable model that best fits the data. Following data analysis, the optimization process was got using the desirability index which provide the information about the needed level of each response with a specified mixture of the determined variables.[37−39] In our designed experiment, the specifications for the desired bilosomal formulation were to minimize Y1 and maximize Y2 and Y3.

Characterization of the Optimized Bilosomal Formulation

Morphology examination of optimized BUD-loaded bilosomal formulation. The morphology of the selected BUD-loaded bilosomal formulation was inspected using transmission electron microscopy (TEM; JEOL, Japan). One drop of the diluted studied sample was placed on a copper grid, left to dry. Then, staining was performed by (1% w/v) phosphotungstic acid, and dried again at room temperature for 10 min prior to TEM visualization.[28]

Differential Scanning Calorimetry (DSC). The thermal properties of CSTRL, SC, Span 60, BUD and the lyophilized optimum BUD-loaded bilosomal formulation were examined using differential scanning calorimeter (Model DSC-50; Shimadzu, Kyoto, Japan). Purified indium (99.9%) was used for apparatus calibration. Samples were accurately weighed (3 mg) and located in standard aluminum pans. Samples were exposed to a gradual heating at a scanning rate of 10°C/min from 10°C to 300°C.[4]

Pharmacological Studies

Wister albino male rats of 140−150 g were obtained from the Animal House of the National Research Centre (Cairo, Egypt). Groups of rats were accommodated under controlled conditions of temperature and light (24±2°C under a 12 h light/dark cycle, respectively). Rats were permitted to free access to water and food (standard laboratory rodent chow). The in vivo study was approved by the Research Ethics Committee, Faculty of Pharmacy, Ahram Canadian University, Cairo, Egypt (No. CEU 422).

Experimental Design. Thirty two rats were randomly allocated in four groups (n = 8). First group was served as the normal group and administered intranasal saline. The second group received PD as a single intranasal dose of 2 mg/kg and was considered as the model of acute lung injury group.[40] Whereas, the third and fourth groups received the market product (Pulmicort®) and the selected BUD-loaded formulation, respectively (0.5 mg/kg; intranasal)[34] for 7 days after PD instillation.

Determination of TNF-α, TGF-β and PKC. Rats were anaesthetized and sacrificed by decapitation. Lung was separated, rinsed with saline and reserved in cold phosphate buffer (pH 7.4). Lung homogenate (20%) was prepared by a homogenizer (Heidolph, DIAX 900, Germany) which was then separated by centrifugation at 4°C and 2000 xg for 20 min. The separated supernatant was stored at -80°C[41] and used for determination of lung contents of TNF-α, TGF-β and PKC using ELISA kits.

Histopathological Assessment

Autopsy samples were taken from the lung of rats in different groups, fixed in 10% formol saline for 24 h, washed with water and dehydrated with serial dilutions of alcohol (methyl, ethyl and absolute ethyl alcohols). Samples were cleared in xylene and placed in paraffin bees wax at 56°C in hot air oven for 24 h. Paraffin tissue blocks were cut by sledge microtome to 4 μm thickness. The obtained tissue sections were collected on glass slides, deparaffinized, stained by hematoxylin & eosin stain for regular examination using light electric microscope[42] (H&E 16 x and 40 x).

Statistical Analysis

The obtained data were expressed as mean ± SD. The statistical significance of differences was analyzed by one way analysis of variance (ANOVA), followed by Tukey's multiple comparisons test using Graph pad Prism software, version 5 (Inc., San Diego, USA). P-values of lower than 0.05 were considered significant.

Results and Discussion

Characterization of BUD-Loaded Bilosomes

Vesicles Size (VS), Polydispersity Index and Zeta Potential

VS plays an important role in determining the in vitro and in vivo performances.[43] The estimated results of the VS for the bilosomal formulations are demonstrated in Table 3. VS-values ranged from 213.3±8.35 to 987.4±60.7 nm. The used software, Design Expert®, permitted the consideration of all studied responses in chorus, it

Table 3
Characterization of the prepared bilosomal vesicles (size, PDI, zeta potential, EE and $Q_{72\,h}$).

Formula	Size (nm)	PDI	Zeta potential (mV)	EE (%)	Q_{72h}(%)
F1	215.9±5.06	0.28	-62.40±0.28	71.96±1.34	98.9±1.90
F2	215.0±4.27	0.26	-62.48±1.80	49.49±3.10	75.9±0.82
F3	419.9±19.8	0.45	-61.72±1.84	85.66±0.56	70.7±2.40
F4	294.4±4.54	0.45	-60.50±0.56	61.17±2.62	49.2±1.62
F5	216.9±3.69	0.46	-56.3±02.26	49.97±0.001	38.4±0.84
F6	213.3±8.35	0.49	-56.97±1.14	46.32±0.01	30.3±1.86
F7	620.7±9.30	0.34	-47.80±0.42	83.77±1.85	25.0±1.13
F8	475.5±38.3	0.49	-54.25±1.92	71.48±1.09	17.6±0.86
F9	539.4±17.3	0.49	-58.94±0.42	34.55±0.03	78.5±3.90
F10	403.6±15.8	0.54	-56.15±0.98	37.80±0.52	65.2±3.66
F11	987.4±60.7	0.44	-50.37±1.32	62.26±3.03	35.2±1.48
F12	638.8±11.0	0.45	-63.38±2.61	44.47±3.95	30.5±1.16
F13	470.8±16.6	0.44	-58.78±1.72	47.50±0.14	53.6±0.80
F14	337.3±18.3	0.45	-63.42±2.0	41.20±1.41	45.3±1.10
F15	571.2±33.6	0.52	-55.07±2.21	61.96±0.06	26.8±0.12
F16	489.1±12.3	0.49	-63.95±0.85	44.96±0.15	18.6±0.80

selects the model that fits the data.[44] The significance level of the tested independent variables on the VS was evaluated by the ANOVA test, and demonstrated the significant effect of all of the studied variables (BUD concentration (A), lipid type (B), and bile salt type (C)) on the VS ($p < 0.05$). Design Expert® plots presenting the impact of factors on the VS are shown in the supplementary file attached (Fig. S1).

As shown in Table 3, vesicles prepared using CSTRL displayed the smallest size significantly compared to those prepared with P 80H, L-α- PC, and L S45. CSTRL gives vesicles of small size and same results were obtained previously.[45−48] This is referred to its ability to stabilize the vesicles, which in turn leads to a decreased tendency of the prepared vesicles to diffuse into each other, resulting in producing vesicles of small size.[17,49]

On the other hand, it was noticed that the increase in PC percentage exerted a decreasing effect on VS. This is related to the increased emulsification power as the amount of PC increases.[50,51] This is clearly manifested in our results as the vesicles prepared with L-α-PC displayed the largest size followed by L S45 then P 80H (percent of PC is 33, 45, and 70, respectively).

P 80H produced vesicles of larger size compared to CSTRL; this was previously demonstrated by Sebaaly *et al.*[15] Whereas the larger vesicles size of L S45 compared to CSTRL could be related to its packing parameter and phase Tm.[52]

The bile salt type exerted an obvious influence on the prepared vesicles' sizes. VS of the bilosomal formulations prepared with SC were larger than those prepared with SDC, similar results were previously obtained.[53,54] This could be due to the greater HLB value of SC (18) compared to HLB value of SDC (16).[54] Larger vesicles are usually produced from surfactants of higher HLB values.[55] This is due to the higher water intake that occurs as HLB values increase, resulting in vesicles of large sizes.[56]

The study also reveals that drug concentration exerted a significant impact on VS. It was observed that by increasing drug concentration, the VS increases. Previous studies had reported a direct relationship that correlates VS with increasing drug concentration.[48,53,57] Higher drug concentration means more drug molecules incorporated within the hydrophobic zones in the vesicles which extend the distances between the vesicular bilayers.[53,57]

The PDI of the prepared bilosomal formulations demonstrated values ranging from 0.26 to 0.54, indicating narrow distribution of size as well as reasonable homogeneity (Table 3). As the PDI-values are small and far from 1, this indicates monodispersed particle population.[58,59]

The prepared bilosomal formulations demonstrated negative charges ranging from -47.80±0.42 to -63.95±0.85 mV, which can indicate the acceptable stability, and that they have adequate charges

that could minimize vesicles aggregation. The presence of the anionic bile salts in the vesicular structure contributed to the resulted negative charges ZP-values.[4,60]

Entrapment Efficiency

Bilosomes are capable of entrapping significant amount of BUD which is considered a prospective feature for its usage as a vesicular carrier. The average EE-values of BUD in different bilosomal formulations ranged from 34.55±0.03 to 85.66±0.56%, as shown in Table 3.

As demonstrated by the ANOVA analysis, all the examined independent variables had a significant effect ($p<0.05$) on the EE% of BUD within the prepared bilosomes; namely: BUD concentration (A), lipid type (B), and type of bile salts (C). Design Expert® plots presenting the impact of factors on the EE are shown in the supplementary file attached (Fig. S1).

The highest EE-values were recorded for BUD-loaded bilosomal formulation prepared using CSTRL as the lipid component (values ranged from 49.49±3.10% to 85.66±0.56%). High drugs EE-values were previously recorded to be associated with the use of CSTRL.[31,45,56,61,62] CSTRL enhances the microviscosity of the vesicular membrane by abolishing the surfactant bilayer's gel-to-liquid phase transition. As a result, a highly-stable hydrophobic bilayer is formed, which prevents drug permeation and consequently hinders its leakage in the bilayer region.[31,45,56] Upon vesicles formation, CSTRL reduces entrapped drug leakage by decreasing vesicles fluidity.[63,64] The elevated membrane mechanical stiffness and cohesion of the vesicles; suggests the capability of the three β-OH head groups of CSTRL to place themselves nearby the sorbitan fatty acid ester groups in the membrane bilayer whereas the lipophilic steroid ring allocating parallel to the used surfactant acyl chains. Furthermore, hydrogen bonds are formed with ester group oxygen atoms of the sorbitan fatty acid enhancing the strength of the bilayers.[64]

Upon comparing the other lipids used, it was found that vesicles prepared using P 80H produced the highest drug EE, followed by those prepared using L S45 and then L-α- PC. Similar drug EE-values ranges for the studied lipids were recorded in earlier studies.[15,48,65,66] It has been previously demonstrated that the concentration of PC directly affects the EE-values.[67,68] The acyl chains of PC offer an encouraging environment for solubilizing hydrophobic drugs. Therefore, the higher the amount of the acyl chains, the higher the entrapped drug amount within the vesicles.[69] Moreover, the increased amount of PC within the vesicles leads to an increase in the bilayers numbers with increased rigidity, and thus, higher drug retaining capacity is produced.[70] This was reflected in the obtained EE-values, which matched the ranking of the contained PC content in the used lipids (70, 45, and 33 for P 80H, L S45, and L-α-PC,

respectively); increasing the PC percent increased the mean EE significantly. The distribution of the drug molecules incorporated within vesicular formulations depends on the physicochemical properties of the drug. The incorporation could be in the following regions: within the internal core phase, into the membrane bilayer, or onto the vesicle membrane.[71] Being a hydrophobic drug, BUD is predicted to be entrapped within the nonpolar lipid bilayer.[72] Thus, the increased amount of PC in the vesicles leads to enhancing the bilayers numbers and rigidity as well as the drug retaining capacity.[70]

Bile salt type exerted a noticeable effect on BUD EE-values. Bilosomes prepared with SC showed higher EE-values than those prepared with SDC. The reason behind this might be related to the higher HLB-value of SC compared to SDC (HLB= 18 and 16, respectively).[31,54,73] The impact of the HLB value indicates that the critical packing parameter of the vesicles should consider the presence of hydrophobic drugs due to their incorporation in the vesicular bilayer.[54] In the current study, the presence of the hydrophobic drug, BUD, could enhance the critical packing parameter for bilayer formation.[74]

The concentration of BUD played a significant role in the obtained EE-values. Bilosomal formulations prepared using a higher initial concentration of BUD demonstrated higher EE-values. Previous studies showed the directly proportional relationship between the initial drug concentration and the resulted EE-values.[54,75−77] This might be attributed to the saturation of the media with BUD, which, in turn, reserves it encapsulated within the formed vesicles.[54,78]

In-Vitro *Drug Release*

This study was performed in order to investigate the influence of various formulation variables on BUD release from the studied vesicular preparations. The release profiles of BUD from the studied vesicular preparations are demonstrated in Fig. 1. As demonstrated in the figure, all of the studied bilosomal formulation exhibited sustained release patterns of BUD, offering an additional advantages over other drug carriers.[18,31] These results indicated that loading BUD into bilosomes could lessen its frequent administration and side effects. By analyzing ANOVA test results, it was found that BUD concentration (A) and lipid type (B) exerted a significant effect ($p < 0.05$) on the release of BUD from the prepared bilosomes. The high affinity of BUD for the hydrophobic components in the bilosomal formulation could be the reason for its slow release.[54] Design Expert® plots presenting the impact of factors on the % RE of BUD from different bilosomal formulations are shown in the supplementary file attached (Fig. S1).

As depicted from Fig. 1, bilosomal formulations prepared using CSTRL demonstrated the highest percentage of drug release. This might be largely related to its smallest VS among the other investigated lipids. Smaller vesicles produce a larger surface area for BUD release. Also, in small-sized vesicles, most of the drug molecules are associated at or near the particles' surfaces leading to faster drug release.[79] On the other hand, it was noted that the drug release showed a faster pattern from L-α-PC-based bilosomes > L S45-based formulations > P 80H-based formulations. It is clearly attributed to the difference in PC percent between them. Increasing the percent of PC decreases the drug release rate; this agrees with former studies.[51, 67,80]

The results of the study revealed the inversely proportional relationship between BUD concentration and its release from the studied formulations. It was noted that as the concentration of drug increase, drug release decrease. A previous study by Guinedi *et al.* demonstrated that formulations with high EE exhibited slower drug release. This might be attributed to entrapping of more drug molecules within the several concentric spheres of lipid bilayers composing the
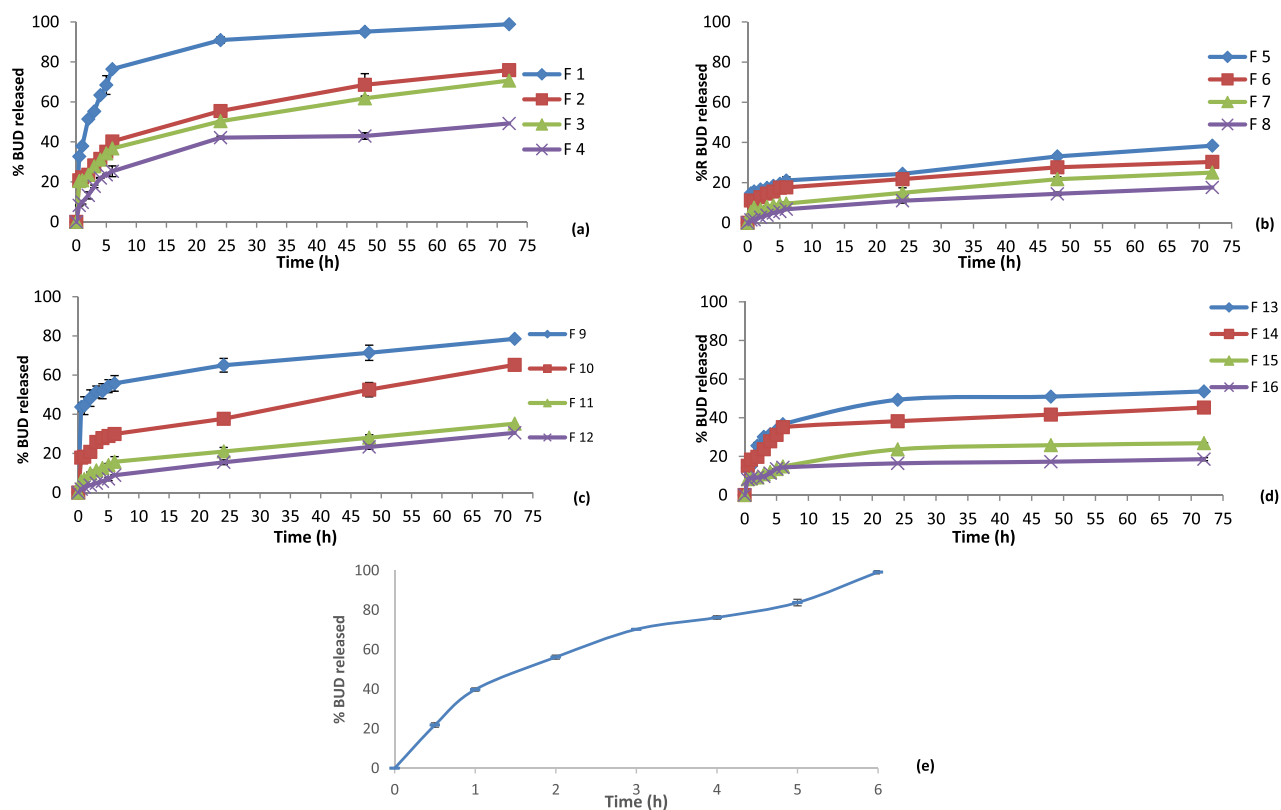

Figure 1. Release profiles of BUD from different bilosomes formulations containing cholesterol (a), phospholipon 80H (b), L-alphaphosphatidylcholine (c), lipid S45 (d), in comparison with free BUD (e) in phosphate buffer (pH=7.4) at 37±0.5°C, mean ±SD, n=3.
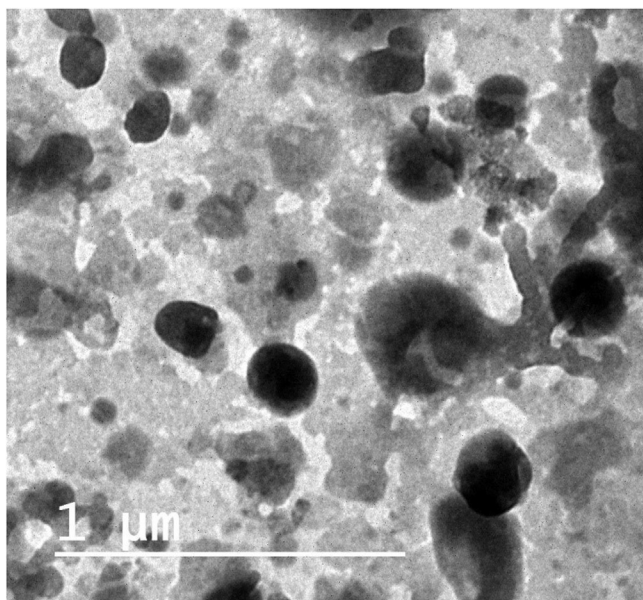
Figure 2. Transmission electron micrograph of the optimized bilosomal formulation (F1).

multilamellar vesicles. This leads to more crowds of drug molecules which hinders their diffusion through the multilamellar vesicles, thus, slowing down the release.[81]

Upon studying BUD release from the vesicular systems (Bilosomes) and comparing it with its free form, the release pattern was slow for the BUD loaded bilosomes (72 h) and fast for free drug (6 h). This sustained release profile of the bilosomal systems may suggest good anti-inflammatory activity and assure its safety.[17,31,82] This improves the therapeutic efficacy so decreases drug's toxicity and adverse effects, and increases patient's compliance with less frequent dosing so improves the quality of life and reduces health care cost.[34, 83]

Optimization

Optimization was performed applying the desirability function which was equal to 0.793, the graph showing the desirability of the prepared formulation is presented in the attached supplementary file (Fig. S2). The bilosomal formulation (F1) attained the smallest VS, reasonable EE-value, and maximum RE-value. Thus, F1 was the formulation of choice for further analysis including its morphology and thermal assessments as well as the *in vivo* study.

Characterizations of the Optimized BUD-Loaded Bilosomal Formulation

Morphology

Morphology of the selected bilosomal system (F1) was manifested by TEM analysis. Images revealed non-aggregating, distinct and spherical vesicles (Fig. 2). There was a good match between the mean VS using the TEM analysis and those obtained from Malvern particle size analyzer.

Differential Scanning Calorimetry

Fig. 3. shows the DSC thermograms of BUD, CSTRL, SC, Span 60, and the optimized bilosomal formulation. DSC study revealed the presence of pure BUD in a crystalline state. The DSC analysis confirms the crystalline character of BUD that exhibited a characteristic melting endotherm at 253.49°C.[84] CSTRL showed endothermic peaks at 147.62°C,[85] SC showed small broad peak at 127.27°C, while Span 60 demonstrated its 3 endothermic peaks at 56.41°C, 124.09°C, and
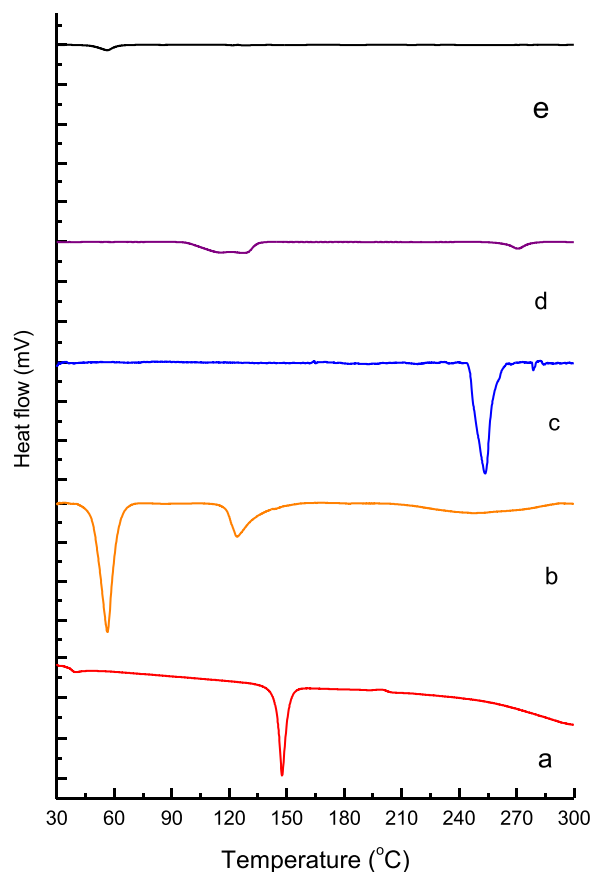

Figure 3. DSC thermograms of (a) cholesterol, (b) span 60, (c) BUD, (d) sodium cholate and (e) lyophilized optimized bilosomal formulation (F1).

247.65°C. In the selected bilosomal system, the complete disappearance of the characteristics BUD peaks indicated that it was completely encapsulated within the formed bilosomes.[17,28,36,86,87]

Pharmacological Effect of Optimized BUD-Loaded Bilosomal Formulation

Effect on lung contents of TNF-α and TGF-β

In the current study, instillation of PD produced an elevation of TNF-α and TGF-β lung contents by 4.8 and 0.6 folds, respectively, upon comparison with the control group data, suggesting that PD induced inflammation and lung injury. The administration of market product (Pulmicort®) and the selected BUD-loaded bilosomal formulation (F1) produced a significant reduction in lung contents of TNF-α by 45% and 78% respectively, TGF-β by 9% and 27% in comparison with those of PD rats. The administration of BUD-loaded bilosomal formulation (F1) decreased lung contents of TNF-α and TGF-β by 59% and 20% respectively, in comparison with those of market product (Pulmicort®) group. In addition, administration of F1 returned TNF-α and TGF-β lung contents to their normal levels as those of the control group (Fig. 4). These results indicated that BUD-loaded bilosomes exhibited a significant effect in decreasing lung inflammation. Thus, inclusion of BUD within bilosomes could boost its therapeutic activity. TNF-α and TGF-β1 stimulation have an important role in acute lung injury via inducing inflammation and releasing ROS which in turn affect bronchioles that become filled by mucous and destruct alveolar walls.[19] Previous studies revealed that BUD decreased TNF-α in Wistar male rats with injured lungs.[88] Another study performed on mice that administered intratracheal lipopolysaccharide to induce acute lung injury showed that the pretreatment with BUD significantly reduced pathological injury, pathological scores, and
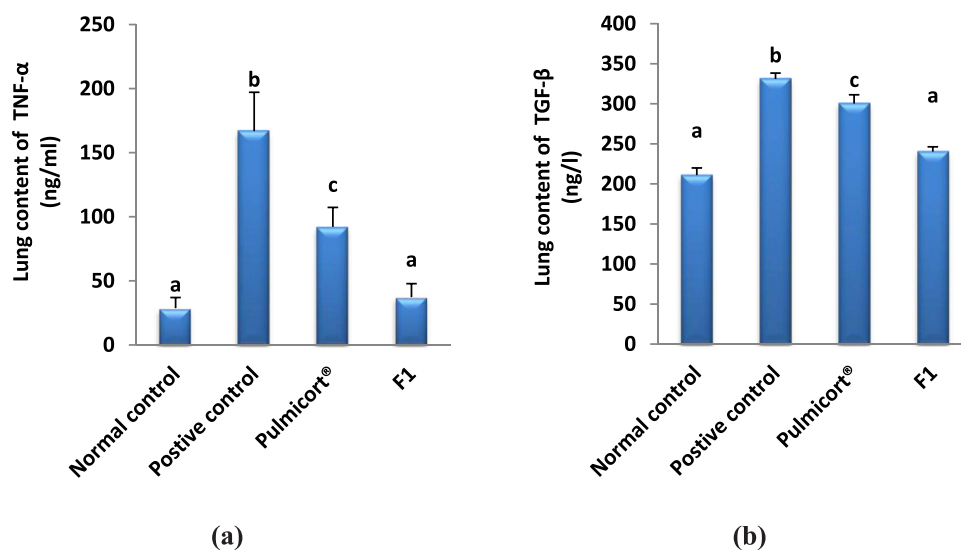
(a) (b)

Figure 4. Effect of Budesonide on TNF-α (a) and TGF-β (b) in the lung Data are presented as the mean $\pm$ SD. of (n=8) for each group. Statistical analysis was carried out by one-way analysis of variance followed by Tukey's multiple comparisons test. Same letter means non-significant difference, while different letter means significant difference at p < 0.05.

decreased TNF-α.[89] Also, BUD modulates airway inflammation induced by ovalbumin aerosol and allergen challenge through controlling TGF-β cytokine.[90] Additionally chronic obstructive pulmonary disease was induced in groups of rats by administration of lipopolysaccharide intratracheally with cigarette smoking, BUD resulted in decreasing TGF-β, and implied its potency against this pulmonary disease.[91] Previous clinical study revealed that nebulized BUD showed significantly improved reduction of inflammatory markers such as TNF-α in respiratory distress patients.[92]

The previous findings reinforced that encapsulation of BUD within the proposed bilosomal carrier as a targeted pulmonary delivery system displayed prolonged BUD release at the desired site with lessened systemic exposure. Therefore, it could be expected to enhance its therapeutic activity. A consequent outcome is to decrease any possible systemic side effects and frequent dosing.[34] The current study could provide a promising evidence for the enhanced efficacy of BUD-loaded bilosomes for relieving acute lung injury.
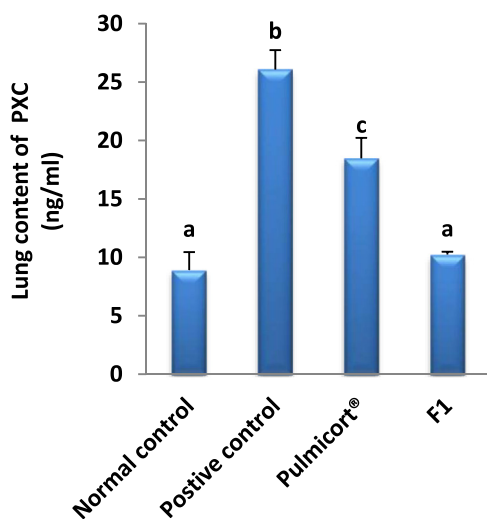

Figure 5. Effect of Budesonide on PKC in the lung Data are presented as the mean $\pm$ SD. of (n=8) for each group. Statistical analysis was carried out by one-way analysis of variance followed by Tukey's multiple comparisons test. Same letter means non-significant difference, while different letter means significant difference at p < 0.05.

Effect on Lung Content of PKC

PKC lung content was elevated by 2 fold in PD group when compared to control group data. The administration of market product (Pulmicort®) and the optimized formulation (F1) decreased PKC lung content by 29% and 61% respectively, as compared to PD group data. The lung contents of PKC was decreased by 45% after treatment with formula as compared to market product (Pulmicort®) group and returned to its normal level as compared to normal control group (Fig. 5).[93] Clinically, BUD exerts an antioxidant activity as it reacts with glucocorticoid receptors in patients with asthma targeting human neutrophils leading to a fast reduction of ROS.[94]

From the previous findings, the superiority of our suggested optimized BUD-loaded bilosomal formulation is clearly perceived as a potent anti-inflammatory agent. The proved boosted activity can be mainly resulted from the enhanced dissolution and penetration of BUD, that, accordingly, could bring about more improved absorption and consequently enhanced bioavailability of BUD. Following their systemic distribution, vesicular systems would lead to improved drug uptake across living tissues by the virtue of their permeability as well as nanometric size.[31] The size of a vesicular carrier exerts a great influence on its in vivo cellular uptake via endocytosis. A previous article by Niu *et al.*[95] stated that vesicles with particle size ranging from 80 to 400 nm demonstrated enhanced cellular uptake as compared to carriers with larger sizes. Endocytosis is an energy dependent process, thus, less energy is required during the process is required for smaller uptake.[95] The delivery of BUD encapsulated within the proposed carrier is expected to treat acute lung injury more efficiently compared to its non-encapsulated form. Encapsulation can confine BUD primarily to lung tissues.[34]

Histopathological Study

Histopathological photos of lung sections from rats of the normal control group showed normal lung structure and normal bronchiole and surrounding air alveoli in the parenchyma (Fig. 6 A&B). The lung of experimentally induced lung injury rats by potassium dichromate showed severe congestion detected in the blood vessels associated with focal perivascular inflammatory cells aggregation surrounding the blood vessels (Fig. 6 C&D), focal inflammatory cells aggregation was detected also in the parenchyma with collapse of the surrounding air alveoli (Fig. 6 E&F). The lung of experimentally induced lung injury rats and treated by commercial form (Pulmicort®) showed
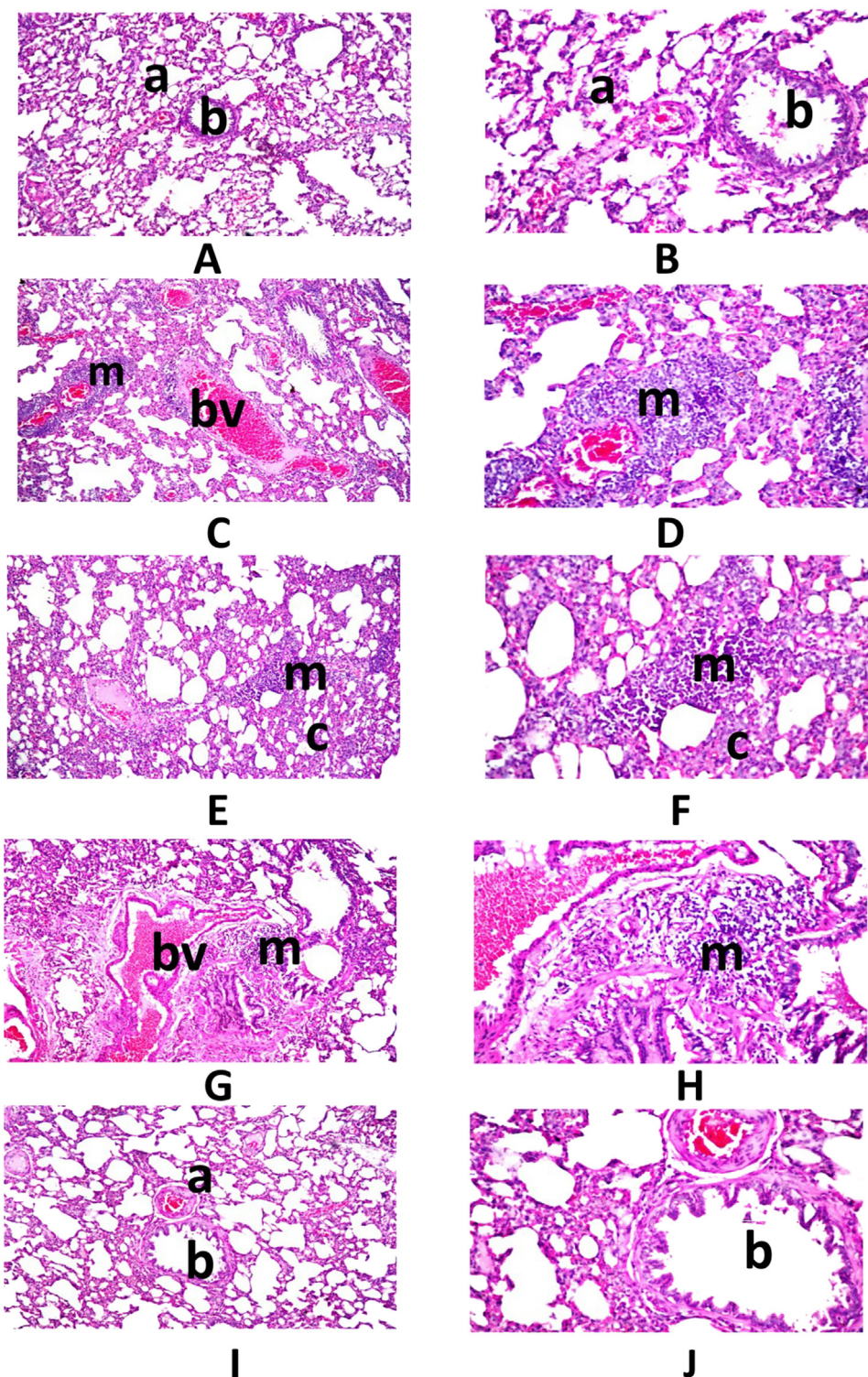
Figure 6. Photomicrographs of histopathological lung sections: A&B: normal control rats, C,D,E&F: PD-induced lung injury (positive control), G&H: PD-induced lung injury and treated by commercial drug (Pulmicort®), I&J: PD-induced lung injury and treated by F1. (H&E, × 16 for A, C, E, G and I; H&E,x40 for B, D, F, H and J). *a: alveoli, b:bronciole, c:collapse, bv: blood vessels, m: inflammatory cell aggregation.

focal few inflammatory cells aggregation in the peribronchiolar tissue associated with congestion in the blood vessels (Fig. 6 G&H). On the other hand, the lung of experimentally induced lung injury rats and treated by F1 showed normal histological structure (Fig. 6 I&J).

In previously published researches, BUD showed significant effect in reducing lung inflammation when lung inflammation induced by ovalbumin in mice[90] and when lung inflammation induced by ventilation in rats[88] and also when lung injury induced by lipopolysaccharide in Wistar rats.[89] More specifically, BUD was found to enhance oxygenation and lung mechanisms when administered by nebulization to patients with acute respiratory distress syndrome, this is associated also with the obvious reduction of the measured inflammation

markers.[92] Being a corticosteroid with anti-inflammatory and immunomodulatory characteristics, BUD is able to constrain early distinctive antiviral immune reactions in vitro, proposing its ability to confine extreme inflammation.[96] Additionally, several clinical trials performed on asthma patients verified the advantageous impact of inhaled BUD on airway inflammation and hyper-responsiveness.[97—99] In a recent study, encouraging results were obtained indicating a promising activity of BUD against SARS-CoV-2 and COVID-19.[2] Moreover, the intranasal inhalation of BUD ameliorated lung injury and decreased uncontrolled inflammation suggesting its effectiveness for the treatment of acute respiratory distress syndrome in clinical practice.[89]

Histopathological results indicated enhanced tissue recovery of rats treated with F1. This could have largely been related to the greater accumulation capacity of bilosomes within the affected inflammatory areas. The histological changes, indicative of inflammatory injury, were noticeably relieved by treatment with BUD-loaded bilosomes, signifying that their rapid and effective healing impact on lung tissues.

The obtained *in vivo* results, assured by the histopathological study, could largely indicate that BUD-loaded bilosomes effectively targeted lung tissues, significantly decreased lung inflammation, extended BUD retention at the targeted site. Hence, it is expected to maximize BUD therapeutic index.

Conclusion

In the presented study, bilosomes were prepared adopting thin film hydration technique. Three independent variables were studied; BUD concentration, type of the used lipid and type of the used bile salt. Upon analyzing the obtained data, an optimized BUD-loaded bilosomal formulation (F1) was selected as it displayed promising results regarding VS (215.9±5.06 nm), EE-values (71.96±1.34%) as well as sustained release characteristics. Morphological assessment by TEM proved the formation of spherical vesicles while DSC study confirmed complete entrapment of BUD within the formed vesicles. To assess the *in vivo* performance of the prepared formulation versus the available market product, a PD-induced acute lung injury in rat model was adopted. Results of the present study provides an experimental evidence for the effect of optimized BUD-loaded bilosomal formulation (F1) on PD-induced acute lung injury in rats via modulation of TGF-β/PKC, and proved its potent effect on treating inflammation as depicted from the histopathogical study. Overall, the obtained data designates that BUD inclusion within the suggested bilosomal system is an auspicious technique to enhance its activity against acute lung injury.

Declaration of Competing Interest

The authors declare that they have no known competing financial interests or personal relationships that could have appeared to influence the work reported in this paper.

Supplementary Materials

Supplementary material associated with this article can be found in the online version at doi:10.1016/j.xphs.2022.10.001.

References

1. Ellul-Micallef R, Hansson E, Johansson S. Budesonide: a new corticosteroid in bronchial asthma. *Eur J Respir Dis*. 1980;61(3):167—173.
2. Heinen N, Meister TL, Klöhn M, Steinmann E, Todt D, Pfaender S. Antiviral effect of budesonide against SARS-CoV-2. *Viruses*. 2021;13(7):1411.
3. Esmaeili M, Aghajani M, Abbasalipourkabir R, Amani A. Budesonide-loaded solid lipid nanoparticles for pulmonary delivery: preparation, optimization, and aerodynamic behavior. *Artif Cells, Nanomed Biotechnol*. 2016;44(8):1964—1971.
4. Al-Mahallawi AM, Abdelbary AA, Aburahma MH. Investigating the potential of employing bilosomes as a novel vesicular carrier for transdermal delivery of tenoxicam. *Int J Pharm*. 2015;485(1-2):329—340.
5. Waglewska E, Pucek-Kaczmarek A, Bazylińska U. Novel surface-modified bilosomes as functional and biocompatible nanocarriers of hybrid compounds. *Nanomaterials*. 2020;10(12):2472.
6. Ahmad R, Srivastava S, Ghosh S, Khare SK. Phytochemical delivery through nanocarriers: a review. *Colloids Surf B*. 2020;111389.
7. He H, Lu Y, Qi J, Zhu Q, Chen Z, Wu W. Adapting liposomes for oral drug delivery. *Acta Pharmaceutica Sinica B*. 2019;9(1):36—48.
8. Chilkawar R, Nanjwade B, Nwaji M, Idris S, Mohamied A. Bilosomes based drug delivery system. *J Chem Appl*. 2015;2(5).
9. Mali N, Darandale S, Vavia P. Niosomes as a vesicular carrier for topical administration of minoxidil: formulation and in vitro assessment. *Drug Deliv Transl Res*. 2013;3(6):587—592.
10. Shinde UA, Kanojiya SS. Serratiopeptidase niosomal gel with potential in topical delivery. *J Pharmaceut*. 2014;2014.
11. Lee S-C, Lee K-E, Kim J-J, Lim S-H. The effect of cholesterol in the liposome bilayer on the stabilization of incorporated retinol. *J Liposome Res*. 2005;15(3-4):157—166.
12. Erdoğ A, Limasale YDP, Keskin D, Tezcaner A, Banerjee S. In vitro characterization of a liposomal formulation of celecoxib containing 1, 2-distearoyl-sn-glycero-3-phosphocholine, cholesterol, and polyethylene glycol and its functional effects against colorectal cancer cell lines. *J Pharm Sci*. 2013;102(10):3666—3677.
13. Janga KY, Tatke A, Balguri SP, et al. Ion-sensitive in situ hydrogels of natamycin bilosomes for enhanced and prolonged ocular pharmacotherapy: in vitro permeability, cytotoxicity and in vivo evaluation. *Artif Cells, Nanomed Biotechnol*. 2018;46 (sup1):1039—1050.
14. Albash R, El-Nabarawi MA, Refai H, Abdelbary AA. Tailoring of PEGylated bilosomes for promoting the transdermal delivery of olmesartan medoxomil: in-vitro characterization, ex-vivo permeation and in-vivo assessment. *Int J Nanomed*. 2019;14:6555.
15. Sebaaly C, Greige-Gerges H, Stainmesse S, Fessi H, Charcosset C. Effect of composition, hydrogenation of phospholipids and lyophilization on the characteristics of eugenol-loaded liposomes prepared by ethanol injection method. *Food Biosci*. 2016;15:1—10.
16. AbouSamra MM, Salama AH. Enhancement of the topical tolnaftate delivery for the treatment of tinea pedis via provesicular gel systems. *J Liposome Res*. 2017;27 (4):324—334.
17. AbouSamra MM, Salama AH, Awad GE, Mansy SS. Formulation and evaluation of novel hybridized nanovesicles for enhancing buccal delivery of ciclopirox olamine. *AAPS PharmSciTech*. 2020;21(7):1—12.
18. Allam A, Fetih G. Sublingual fast dissolving niosomal films for enhanced bioavailability and prolonged effect of metoprolol tartrate. *Drug Des Dev Ther*. 2016;10:2421.
19. Salama A, Fayed HM, Elgohary R. L-carnitine alleviated acute lung injuries induced by potassium dichromate in rats: involvement of Nrf2/HO-1 signaling pathway. *Heliyon*. 2021;7(6).
20. Salama A, Elsayeh B, Ismaiel I, El-Shenawy S. Comparative evaluation of protective effects of green tea and lycopene in potassium dichromate-induced acute renal failure in rats. *J Chem Pharm Res*. 2014;6(12):168—177.
21. Salama A, Mostafa R, Omara E. Ameliorative effects of phosphodiesterase (PDE) inhibitors in potassium dichromate-induced acute renal failure in rats. *Int J Pharm Sci Rev Res*. 2016;36(2):40—46.
22. Hegazy R, Salama A, Mansour D, Hassan A. Renoprotective effect of lactoferrin against chromium-induced acute kidney injury in rats: involvement of IL-18 and IGF-1 inhibition. *PLoS One*. 2016;11(3): e0151486.
23. Cho SC, Rhim JH, Choi HR, et al. Protective effect of 4, 4'-diaminodiphenylsulfone against paraquat-induced mouse lung injury. *Exp Mol Med*. 2011;43(9):525—537.
24. Asrani P, Hassan MI. SARS-CoV-2 mediated lung inflammatory responses in host: targeting the cytokine storm for therapeutic interventions. *Mol Cell Biochem*. 2021;476(2):675—687.
25. Huang C, Wang Y, Li X, et al. Clinical features of patients infected with 2019 novel coronavirus in Wuhan, China. *Lancet North Am Ed*. 2020;395(10223):497—506.
26. Naqvi AAT, Fatima K, Mohammad T, et al. Insights into SARS-CoV-2 genome, structure, evolution, pathogenesis and therapies: structural genomics approach. *Biochimica et Biophysica Acta (BBA)-Mol Basis Dis*. 2020;1866(10): 165878.
27. Poduri R, Joshi G, Jagadeesh G. Drugs targeting various stages of the SARS-CoV-2 life cycle: exploring promising drugs for the treatment of Covid-19. *Cell Signall*. 2020;74: 109721.
28. Ahmed S, Kassem MA, Sayed S. Bilosomes as promising nanovesicular carriers for improved transdermal delivery: construction, in vitro optimization, ex vivo permeation and in vivo evaluation. *Int J Nanomed*. 2020;15:9783.
29. El-Nabarawi M, Nafady M, Elmenshawe S, Elkarmalawy M, Teaima M. Liver targeting of daclatasvir via tailoring sterically stabilized bilosomes: fabrication, comparative in vitro/in vivo appraisal and biodistribution studies. *Int J Nanomed*. 2021;16:6413.
30. Salem HF, Ali AA, Hegazy AM, Sadek A-RA, Aboud HM. Harnessing of doxylamine succinate/pyridoxine hydrochloride-dual laden bilosomes as a novel combinatorial nanoparadigm for intranasal delivery: in vitro optimization and in vivo pharmacokinetic appraisal. *J Pharm Sci*. 2022;111(3):794—809.

31. Matloub AA, Salama AH, Aglan HA, AbouSamra MM, ElSouda SSM, Ahmed HH. Exploiting bilosomes for delivering bioactive polysaccharide isolated from Enteromorpha intestinalis for hacking hepatocellular carcinoma. *Drug Dev Ind Pharm*. 2018;44(4):523−534.

32. Habib BA, Sayed S, Elsayed GM. Enhanced transdermal delivery of ondansetron using nanovesicular systems: fabrication, characterization, optimization and ex-vivo permeation study-Box-Cox transformation practical example. *Eur J Pharm Sci*. 2018;115:352−361.

33. Mahmoud AA, Salama AH, Shamma RN, Farouk F. Bioavailability enhancement of aripiprazole via silicosan particles: Preparation, characterization and in vivo evaluation. *AAPS PharmSciTech*. 2018;19(8):3751−3762.

34. Chennakesavulu S, Mishra A, Sudheer A, Sowmya C, Reddy CS, Bhargav E. Pulmonary delivery of liposomal dry powder inhaler formulation for effective treatment of idiopathic pulmonary fibrosis. *Asian J Pharm Sci*. 2018;13(1):91−100.

35. Salama AH, AbouSamra MM, Awad GE, Mansy SS. Promising bioadhesive ofloxacin-loaded polymeric nanoparticles for the treatment of ocular inflammation: formulation and in vivo evaluation. *Drug Deliv Transl Res*. 2021;11(5):1943−1957.

36. Gupta AS, Kshirsagar SJ, Bhalekar MR, Saldanha T. Design and development of liposomes for colon targeted drug delivery. *J Drug Targeting*. 2013;21(2):146−160.

37. Salem HF, Kharsoum RM, El-Ela FIA, Abdellatif KR. Evaluation and optimization of pH-responsive niosomes as a carrier for efficient treatment of breast cancer. *Drug Deliv Transl Res*. 2018;8(3):633−644.

38. Ammar HO, Ghorab M, Kamel R, Salama AH. Design and optimization of gastro-retentive microballoons for enhanced bioavailability of cinnarizine. *Drug Deliv Transl Res*. 2016;6(3):210−224.

39. Ammar HO, Ghorab M, Kamel R, Salama AH. A trial for the design and optimization of pH-sensitive microparticles for intestinal delivery of cinnarizine. *Drug Deliv Transl Res*. 2016;6(3):195−209.

40. Salama A, Hegazy R, Hassan A. Intranasal chromium induces acute brain and lung injuries in rats: assessment of different potential hazardous effects of environmental and occupational exposure to chromium and introduction of a novel pharmacological and toxicological animal model. *PLoS One*. 2016;11(12): e0168688.

41. Salama AA, Zaki HF, Siham M, EL-Denshary E, Ismaiel IE-K. Antiasthmatic effects of evening primrose oil in ovalbumin-allergic rats. *Pharm Lett*. 2015;7:214−223.

42. Banchroft J, Stevens A, Turner D. *Theory and Practice of Histological Techniques*. New York, London, San Francisco, Tokyo: Churchil Livingstone; 1996.

43. Sun W, Zou W, Huang G, Li A, Zhang N. Pharmacokinetics and targeting property of TFu-loaded liposomes with different sizes after intravenous and oral administration. *J Drug Target*. 2008;16(5):357−365.

44. Salem HF, Kharsoum RM, Sayed OM, Abdel Hakim LF. Formulation design and optimization of novel soft glycerosomes for enhanced topical delivery of celecoxib and cupferron by Box-Behnken statistical design. *Drug Dev Ind Pharm*. 2018;44(11):1871−1884.

45. Mokhtar M, Sammour OA, Hammad MA, Megrab NA. Effect of some formulation parameters on flurbiprofen encapsulation and release rates of niosomes prepared from proniosomes. *Int J Pharm*. 2008;361(1-2):104−111.

46. Mirzaei-Parsa MJ, Najafabadi MRH, Haeri A, et al. Preparation, characterization, and evaluation of the anticancer activity of Artemether-loaded Nano-Niosomes against breast cancer. *Breast Cancer*. 2020;27(2):243−251.

47. Gaur PK, Purohit S, Kumar Y, Mishra S, Bhandari A. Ceramide-2 nanovesicles for effective transdermal delivery: development, characterization and pharmacokinetic evaluation. *Drug Dev Ind Pharm*. 2014;40(4):568−576.

48. El Menshawe SF, Aboud HM, Elkomy MH, Kharsoum RM, Abdeltwab AM. A novel nanogel loaded with chitosan decorated bilosomes for transdermal delivery of terbutaline sulfate: artificial neural network optimization, in vitro characterization and in vivo evaluation. *Drug Deliv Transl Res*. 2020;10(2):471−485.

49. Ya'akob HB, Chin CS, Abd Aziz A, et al. Effect of span 60, Labrasol, and cholesterol on Labisia pumila loaded niosomes quality. *Int J Biotechnol Bioeng*. 2017;11(7):521−524.

50. Abd-Elsalam WH, El-Helaly SN, Ahmed MA, Al-Mahallawi AM. Preparation of novel phospholipid-based sonocomplexes for improved intestinal permeability of rosuvastatin: in vitro characterization, dynamic simulation, Caco-2 cell line permeation and in vivo assessment studies. *Int J Pharm*. 2018;548(1):375−384.

51. Chen J, Ping Q, Guo J, Chu X, Song M. Effect of phospholipid composition on characterization of liposomes containing 9-nitrocamptothecin. *Drug Dev Ind Pharm*. 2006;32(6):719−726.

52. Jovanović AA, Balanč BD, Ota A, et al. Comparative effects of cholesterol and β-sitosterol on the liposome membrane characteristics. *Eur J Lipid Sci Technol*. 2018;120(9): 1800039.

53. El-Nabarawi MA, Shamma RN, Farouk F, Nasralla SM. Bilosomes as a novel carrier for the cutaneous delivery for dapsone as a potential treatment of acne: preparation, characterization and in vivo skin deposition assay. *J Liposome Res*. 2020;30(1):1−11.

54. Mohsen AM, Asfour MH, Salama AA. Improved hepatoprotective activity of silymarin via encapsulation in the novel vesicular nanosystem bilosomes. *Drug Dev Ind Pharm*. 2017;43(12)):2043−2054.

55. Yoshioka T, Sternberg B, Florence AT. Preparation and properties of vesicles (niosomes) of sorbitan monoesters (Span 20, 40, 60 and 80) and a sorbitan triester (Span 85). *Int J Pharm*. 1994;105(1):1−6.

56. Manosroi A, Wongtrakul P, Manosroi J, et al. Characterization of vesicles prepared with various non-ionic surfactants mixed with cholesterol. *Colloids Surf B*. 2003;30(1-2):129−138.

57. Hathout RM, Mansour S, Mortada ND, Guinedi AS. Liposomes as an ocular delivery system for acetazolamide: in vitro and in vivo studies. *Aaps Pharmscitech*. 2007;8(1):E1−E12.

58. Shamma RN, Elsayed I. Transfersomal lyophilized gel of buspirone HCl: formulation, evaluation and statistical optimization. *J Liposome Res*. 2013;23(3):244−254.

59. Salama AH, Basha M, Salama AA. Micellar buccal film for safe and effective control of seizures: preparation, in vitro characterization, ex vivo permeation studies and in vivo assessment. *Eur J Pharm Sci*. 2021;166: 105978.

60. Abdelkader H, Ismail S, Kamal A, Alany RG. Design and evaluation of controlled-release niosomes and discomes for naltrexone hydrochloride ocular delivery. *J Pharm Sci*. 2011;100(5):1833−1846.

61. Gaur PK, Purohit S, Kumar Y, Mishra S, Bhandari A. Preparation, characterization and permeation studies of a nanovesicular system containing diclofenac for transdermal delivery. *Pharm Dev Technol*. 2014;19(1):48−54.

62. Jhan S, Pethe AM. Double-loaded liposomes encapsulating lycopene β-cyclodextrin complexes: preparation, optimization, and evaluation. *J Liposome Res*. 2020;30(1):80−92.

63. Abdelbary G, El-Gendy N. Niosome-encapsulated gentamicin for ophthalmic controlled delivery. *AAPS Pharmscitech*. 2008;9(3):740−747.

64. Nasseri B. Effect of cholesterol and temperature on the elastic properties of niosomal membranes. *Int J Pharm*. 2005;300(1-2):95−101.

65. Ahad A, Raish M, Ahmad A, Al-Jenoobi FI, Al-Mohizea AM. Development and biological evaluation of vesicles containing bile salt of telmisartan for the treatment of diabetic nephropathy. *Artif Cells, Nanomed Biotechnol*. 2018;46(sup1):532−539.

66. Mura P, Maestrelli F, González-Rodríguez ML, Michelacci I, Ghelardini C, Rabasco AM. Development, characterization and in vivo evaluation of benzocaine-loaded liposomes. *Eur J Pharm Biopharm*. 2007;67(1):86−95.

67. El-Menshawe SF, Ali AA, Halawa AA, El-Din ASS. A novel transdermal nanoethosomal gel of betahistine dihydrochloride for weight gain control: in-vitro and in-vivo characterization. *Drug Des Dev Ther*. 2017;11:3377.

68. Ahmad I, Arsalan A, Ali SA, et al. Formulation and stabilization of riboflavin in liposomal preparations. *J Photochem Photobiol, B*. 2015;153:358−366.

69. El-Nabarawi MA, Shamma RN, Farouk F, Nasralla SM. Dapsone-loaded invasomes as a potential treatment of acne: preparation, characterization, and in vivo skin deposition assay. *Aaps Pharmscitech*. 2018;19(5):2174−2184.

70. Abdel Messih HA, Ishak RA, Geneidi AS, Mansour S. Nanoethosomes for transdermal delivery of tropisetron HCl: multi-factorial predictive modeling, characterization, and ex vivo skin permeation. *Drug Dev Ind Pharm*. 2017;43(6):958−971.

71. Shen L-N, Zhang Y-T, Wang Q, Xu L, Feng N-P. Enhanced in vitro and in vivo skin deposition of apigenin delivered using ethosomes. *Int J Pharm*. 2014;460(1-2):280−288.

72. Chourasia MK, Kang L, Chan SY. Nanosized ethosomes bearing ketoprofen for improved transdermal delivery. *Results Pharma Sci*. 2011;1(1):60−67.

73. Lenherr G, Csaba N, Thwala NL, Niu Z, and Alonso MJ, *Nanocapsular formulation of active pharmaceutical ingredients*. 2017, Google Patents.

74. Uchegbu IF, Vyas SP. Non-ionic surfactant based vesicles (niosomes) in drug delivery. *Int J Pharm*. 1998;172(1-2):33−70.

75. Gharib R, Greige-Gerges H, Fourmentin S, Charcosset C. Hydroxypropyl-ß-cyclodextrin as a membrane protectant during freeze-drying of hydrogenated and non-hydrogenated liposomes and molecule-in-cyclodextrin-in-liposomes: application to trans-anethole. *Food Chem*. 2018;267:67−74.

76. Sebaaly C, Jraij A, Fessi H, Charcosset C, Greige-Gerges H. Preparation and characterization of clove essential oil-loaded liposomes. *Food Chem*. 2015;178:52−62.

77. Risaliti L, Ambrosi M, Calamante M, Bergonzi MC, Nostro PL, Bilia AR. Preparation and characterization of ascosome vesicles loaded with Khellin. *J Pharm Sci*. 2020;109(10):3114−3124.

78. El-Samaligy M, Afifi N, Mahmoud E. Increasing bioavailability of silymarin using a buccal liposomal delivery system: preparation and experimental design investigation. *Int J Pharm*. 2006;308(1-2):140−148.

79. Mohanraj V, Chen Y. Nanoparticles-a review. *Trop J Pharmaceut Res*. 2006;5(1):561−573.

80. Agnihotri SA, Soppimath KS, Betageri GV. Controlled release application of multilamellar vesicles: a novel drug delivery approach. *Drug Deliv*. 2010;17(2):92−101.

81. Guinedi AS, Mortada ND, Mansour S, Hathout RM. Preparation and evaluation of reverse-phase evaporation and multilamellar niosomes as ophthalmic carriers of acetazolamide. *Int J Pharm*. 2005;306(1-2):71−82.

82. Yousry C, Zikry PM, Salem HM, Basalious EB, El-Gazayerly ON. Integrated nanovesicular/self-nanoemulsifying system (INV/SNES) for enhanced dual ocular drug delivery: statistical optimization, in vitro and in vivo evaluation. *Drug Deliv Transl Res*. 2020;10(3):801−814.

83. Rizvi SA, Saleh AM. Applications of nanoparticle systems in drug delivery technology. *Saudi Pharmaceut J*. 2018;26(1):64−70.

84. Bhatt H, Naik B, Dharamsi A. Solubility enhancement of budesonide and statistical optimization of coating variables for targeted drug delivery. *J Pharmaceut*. 2014;2014.

85. Rahman SA, Abdelmalak NS, Badawi A, Elbayoumy T, Sabry N, Ramly AE. Formulation of tretinoin-loaded topical proniosomes for treatment of acne: in-vitro characterization, skin irritation test and comparative clinical study. *Drug Deliv*. 2015;22(6):731−739.

86. Martin TM, Bandi N, Shulz R, Roberts CB, Kompella UB. Preparation of budesonide and budesonide-PLA microparticles using supercritical fluid precipitation technology. *AAPS PharmSciTech*. 2002;3(3):16−26.

87. Khalil RM, Abdelbary A, Kocova El-Arini S, Basha M, El-Hashemy HA. Evaluation of bilosomes as nanocarriers for transdermal delivery of tizanidine hydrochloride: in vitro and ex vivo optimization. *J Liposome Res*. 2019;29(2):171−182.

88. Ju YN, Yu KJ, Wang GN. Budesonide ameliorates lung injury induced by large volume ventilation. *BMC Pulm Med*. 2016;16(1):90.

89. Dong L, Zhu Y-H, Liu D-X, et al. Intranasal application of budesonide attenuates lipopolysaccharide-induced acute lung injury by suppressing nucleotide-binding oligomerization domain-like receptor family, pyrin domain-containing 3 inflammasome activation in mice. *J Immunol Res*. 2019;2019.

90. McMillan SJ, Xanthou G, Lloyd CM. Therapeutic administration of Budesonide ameliorates allergen-induced airway remodelling. *Clin Exp Allergy*. 2005;35(3):388–396.

91. Wu DQ, Liu J, Lu XY, Shen HH. [The expression of transforming growth factor beta-1 in rat model of chronic obstructive pulmonary disease and the effects of early drugs intervention]. *Zhejiang Da Xue Xue Bao Yi Xue Ban*. 2004;33(5): 448.

92. Mohamed HS, Meguid MMA. Effect of nebulized budesonide on respiratory mechanics and oxygenation in acute lung injury/acute respiratory distress syndrome: randomized controlled study. *Saudi J Anaesthesia*. 2017;11(1):9.

93. Pan NY, Hui WS, Tipoe GL, et al. Inhibition of pyocyanin-potentiated IL-8 release by steroids in bronchial epithelial cells. *Respir Med*. 2006;100(9):1614–1622.

94. Braga PC, Dal Sasso M, Culici M, Bianchi T, Guffanti EE. Budesonide reduces super-oxide and peroxynitrite anion chemiluminescence during human neutrophil bursts. *Pharmacology*. 2005;75(4):179–186.

95. Niu M, Tan Yn, Guan P, et al. Enhanced oral absorption of insulin-loaded liposomes containing bile salts: a mechanistic study. *Int J Pharm*. 2014;460(1-2):119–130.

96. Davies JM, Carroll ML, Li H, et al. Budesonide and formoterol reduce early innate anti-viral immune responses in vitro. *PLoS One*. 2011;6(11):e27898.

97. Gibson PG, Saltos N, Fakes K. Acute anti-inflammatory effects of inhaled budesonide in asthma: a randomized controlled trial. *Am J Respir Crit Care Med*. 2001;163(1):32–36.

98. Becky Kelly EA, Busse WW, Jarjour NN. Inhaled budesonide decreases airway inflammatory response to allergen. *Am J Respir Crit Care Med*. 2000;162(3):883–890.

99. Mendes ES, Rebolledo P, Campos M, Wanner A. Immediate antiinflammatory effects of inhaled budesonide in patients with asthma. *Ann Am Thoracic Soc*. 2014;11(5):706–711.